archaeometry

Archaeometry ••, •• (2012) ••–•• doi: 10.1111/j.1475-4754.2012.00732.x

COMPOSITIONAL ANALYSES OF MORTARS FROM THE LATE ANTIQUE SITE OF SON PERETÓ (MALLORCA, BALEARIC ISLANDS, SPAIN): ARCHAEOLOGICAL IMPLICATIONS*

D. MIRIELLO,† A. BLOISE and G. M. CRISCI

Università della Calabria, Dipartimento di Scienze della Terra, Via P. Bucci cubo 15B, Arcavacata di Rende (CS), 87036 Calabria, Italy

M. Á. CAU ONTIVEROS

Institució Catalana de Recerca i Estudis Avançats (ICREA)/director of ERAAUB, Universitat de Barcelona/Scientific director of the archaeological excavations of Son Peretó, Facultat de Geografia i Història, Departament de Prehistòria, Història Antiga i Arqueologia, c/ Montalegre, 6–8, 08001 Barcelona, Spain

A. PECCI

Equip de Recerca Arqueològica i Arqueomètrica, Universitat de Barcelona (ERAAUB), Facultat de Geografia i Història, Departament de Prehistòria, Història Antiga i Arqueologia, c/ Montalegre, 6–8, 08001 Barcelona, Spain

and M. RIERA RULLAN

Archaeologist, Technical director of the archaeological excavations of Son Peretó, Cala Mitjana 10, 07009 Palma, Illes Balears, Spain

The paper presents the mineralogical, petrographic and chemical analyses of mortars from an Early Christian complex found in Mallorca (Balearic Islands) and dated to between the fifth and the eighth centuries AD. *We characterized several mortars found at the site, in order to gather information on the raw materials used, as well as on the technology of production, and similarities among the samples. The analyses were aimed at solving specific archaeological questions regarding the building phases of the site and, in particular, the synchronic or diachronic presence of two baptismal basins in the same Christian complex.*

KEYWORDS: BINDER, MORTARS, SEM–EDS, OM, XRPD, XRF, LATE ANTIQUITY

INTRODUCTION

The Balearic Islands were a province of the Roman Empire in the fourth century AD. In AD 455, they became part of the *Regnum Vandalorum*, and in AD 534, after the defeat of the Vandals by Belisarius, they entered the Byzantine Empire, which lasted, theoretically, until 902–3, when the Muslims conquered the islands. One of the main aspects of this vast period was the rise and consolidation of Christendom. The main architectural evidence of early Christianity is represented by a series of basilicas, among which some were excavated. One of the best examples is the so-called Basilica of Son Peretó (Manacor) in the eastern part of Mallorca (Fig. 1 (a)). Occupied mainly between the fifth and the eighth centuries (Riera *et al*. 2006, 2010), the site of

*Received 15 March 2012; accepted 10 April 2012
†Corresponding author: email miriello@unical.it

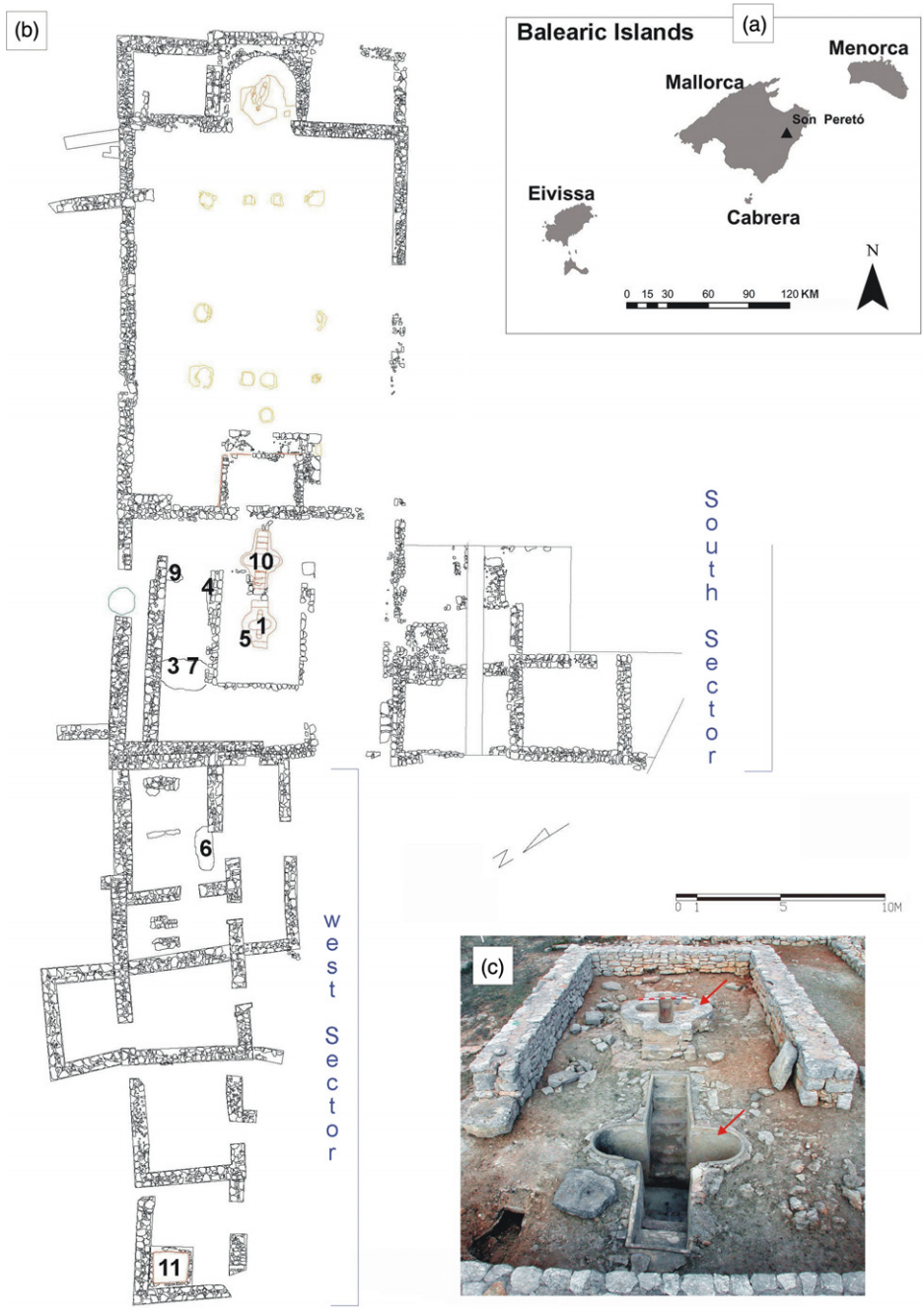

Figure 1 *(a) The location of Son Peretó. (b) The structure of the archaeological site and points of sampling. (c) The baptismal basins.*

Son Peretò is a good example of an Early Christian complex (Fig. 1 (b)) and one of the most important sites for the understanding of the Early Byzantine period in the island.

The discovery dates back to 1912, when Aguiló uncovered different parts of the site, including the basilica and the baptistery (Aguiló 1923). Iturgáiz also investigated the baptistery (Iturgáiz 1963). The site attracted the attention of Palol and his colleagues, who excavated the area in the late 1960s; in particular, the baptistery and the western part of the church (Palol 1967; Palol *et al*. 1967). They also studied the mosaics found in old excavations, attempting a reconstruction of the mosaics' disposition in the different spaces in the church. The work also included the restoration of different parts of the site. It was not until the 1980s that an extensive excavation, directed by G. Rosselló, P. Palol and M. Orfila, was carried out, uncovering many parts of the so-called West Sector.

All this archaeological research allowed the discovery of a Christian church with a baptistery in the western part and several associated rooms both westwards and southwards of the religious buildings (Fig. 1 (c)). The basilica is a three-naved building with an apse that is square outside and semicircular inside. Both sides of the *presbyterium* have attached rooms that seem to belong to a later phase of the building, forming a tripartite apse. The church was paved with mosaics during some of its building phases. A baptistery was attached to the basilica westwards, with the particularity of the presence of two different baptismal fonts.

In 2005, a new project was undertaken in order to restore the site, which was in a progressive state of abandonment. The main goal was to re-excavate the parts already affected by previous archaeological works, to carry out the consolidation and restoration, and to prepare the site as a museum in order to open it to the public (Riera *et al*. 2006, 2010). In addition, the project was aimed at solving some of the scientific problems that were still unsolved, including the problem of the construction phases and the presence of two baptismal fonts in the same baptistery. To do so, an archaeological excavation was carried out together with an analytical programme, including a pilot archaeometric characterization of mortars and plasters.

The study of mortars and plasters, artificial mixtures of a binder (mainly lime), sand and water, may indeed help to solve important technological, archaeological and historical problems. The mineralogical and chemical composition of the aggregates and binder can produce mixtures with very different technological characteristics. The latter were used to establish different construction phases in the buildings and/or the presence of different groups of workers who attended the construction of the monuments. In general, it is possible to affirm that samples with the same compositional and textural features may belong to the same construction phase and may have been produced by the same labour force (Vendrell-Saz *et al*. 1996; Cagnana and Mannoni 2000; Crisci *et al*. 2001, 2004; Moropoulou *et al*. 2003; Crisci and Miriello 2006; Carò *et al*. 2008; Miriello *et al*. 2010b). The study of mortars and plasters may supply information on the provenance of the raw materials used to make them, as well as on the technology of manufacture (Moropoulou *et al*. 1995; Vendrell-Saz *et al*. 1996; Bakolas *et al*. 1998; Crisci *et al*. 2004; Meir *et al*. 2005; Anastasiou *et al*. 2006; Miriello and Crisci 2006; Riccardi *et al*. 2007; Miriello *et al*. 2010a,b, 2011a,b; Regev *et al*. 2010; Iordanidis *et al*. 2011).

The present paper presents the results of a relatively small-scale archaeometric study aiming at solving an important problem related to liturgical issues due to the presence of two baptismal fonts in the same baptistery, which could have been used contemporaneously. One of the baptismal fonts is 1.10 m deep and has a cruciform plan formed by an east–west (2.95 m) rectangular arm with four steps on each side, and a shorter axis north–south (1.85 m) with rounded edges. The second baptismal font is smaller and only 0.56 m deep, with two arms with rounded edges of 1.40 m (east–west) and 1.05 m (north–south). The presence of two baptismal

fonts in the same baptistery is rare and their contemporary use would be strange, particularly when one considers that the two fonts are very different in size. The fact that the original old excavations, during which the fonts were uncovered, did not pay particular attention to the stratigraphical sequence has not allowed a reliable relative chronology to be fixed for the two baptismal fonts. Therefore, the subject has raised some debates—which are still open—regarding the contemporaneity of the fonts (Godoy 1989; Duval 1994; Palol 1994; Godoy 1995; Alcaide 2011—see especially Godoy 1995, 161). The hypothesis sustained by the current archaeological team is that the larger basin could have been used earlier for immersion baptism of adults, while the second font, which is smaller, could have been used later, when infant baptism became more common. Although new archaeological data from the re-excavation of the baptistery and liturgical considerations make this hypothesis plausible, there was no objective proof of this. The study of the mortars of the two basins was aimed at establishing similarities and dissimilarities between the two, on a firmer basis, considering that the use of the same mortar for the two fonts could have been an indication of their construction during the same phase and of the possibility of their simultaneous use. Furthermore, in a recent archaeological project, the small basin was lifted, allowing excavations to take place underneath it. Surprisingly, broken fragments of a baptismal font were recovered. These fragments could be part of the larger basin itself or part of a different one. If the archaeometric study could identify these fragments as part of the larger basin, this would mean that it was partially dismantled and some fragments used as a filling for the construction of the smaller one. If so, the pre-existence of the larger basin would be demonstrated, thus finally closing the debate on the possible contemporary use of two baptismal fonts of different sizes in the same baptistery.

Due to this particular question, most of the samples were taken from different parts of the baptistery (Table 1 and Fig. 1). The objective was to characterize the samples themselves, to identify the raw materials employed and to verify whether there were similarities among the samples—in particular, between the two fonts. The analyses of the other samples focused, as a first insight, on the building techniques and the raw materials used. Moreover, they were aimed at detecting any similarities between the archaeological samples that could allow a better

Table 1 *Analysed samples from Son Peretó*

Sample	*Stratigraphic unit*	*Description*
01		Mortar from the small baptismal basin
03	241	A fragment of a mortar found in the superficial infilling of burial 2008-6, found in the northern room of the baptistery
04	323	Mortar from the cover of a tomb found under the wall that divides the central and the northern rooms of the baptistery
05	271	Mortar fragments found under the small baptismal basin
06	34	Mortar from the cover of tomb 2008-1 in room II of sector W
07	262	A fragment of a mortar found in the infilling of burial 2008-6, found in the northern room of the baptistery
09	307	Mortar from the remains of a floor in the northern room of the baptistery
10		Mortar from the large baptismal basin
11	184–6	Mortar from a basin for production activities from sector W

understanding of the building sequence of the site. Samples of mortars were recovered either *in situ*, from the coatings of basins, floors and covers of tombs, or as fragments in the infilling of other sediments.

MATERIALS AND METHODS

Materials

A total of seven samples were taken from different parts of the baptistery (Table 1 and Fig. 1 (b)). Sample 01 comes from the so-called 'small baptismal basin' (Fig. 1 (c)). In thin section, the sample has two layers: the thinner and inner layer was called 01_I (Fig. 2), while the thicker and external layer was called 01_II (Fig. 2). Sample 10 comes from the wall of the so-called 'large baptismal basin'. It has two layers: the thinner layer was called 10_I, while the thicker, external layer was called 10_II (Fig. 3). Sample 05 is a fragment of *opus signinum* (crushed ceramics mixed with lime) that was recovered from under the so-called 'small basin'. Sample 05 has two layers, the thicker external layer being called 05_II (Fig. 4), while the thinner layer was called 05_I (Fig. 4). This mortar could belong either to the partially dismantled larger basin (sample 10) or to a more ancient basin, that was destroyed in order to build the smaller one (sample 01). The analysis of this set of samples was carried out in order to solve the question of the possible contemporaneity of the baptismal basins. Sample 03 was taken from the superficial infilling of burial 2008-6, which was found in the room to the north of the baptistery. Sample 07 comes from a lower infilling of the same tomb. Both samples have a single layer. Sample 04 was recovered from the mortar of the cover of a tomb found under the wall that divides the central and the northern rooms of the baptistery, while sample 09 was taken from a floor of the northern room of the baptistery. The two samples have a single layer. Together with these two samples, sample 06—which comes from the plastered cover of tomb 2008-1, in sector W, room II—was taken because it provides a good *terminus post quem* of around AD 500 due to the presence of African Red Slip Ware form Hayes 99. A second sample (sample 11)—which does not come from the baptistery—was taken from the plastered coating of a basin that was found in room VII of sector W (Fig. 1), because it had a hydraulic mortar.

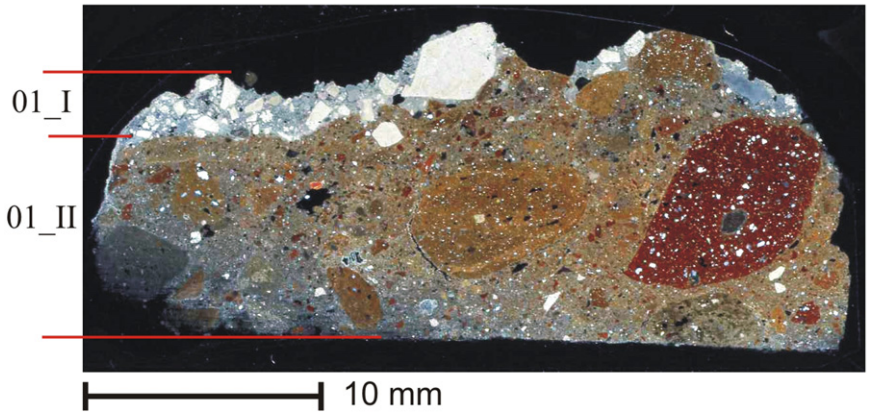

Figure 2 *A flatbed scanner image of sample 01 (crossed polars).*

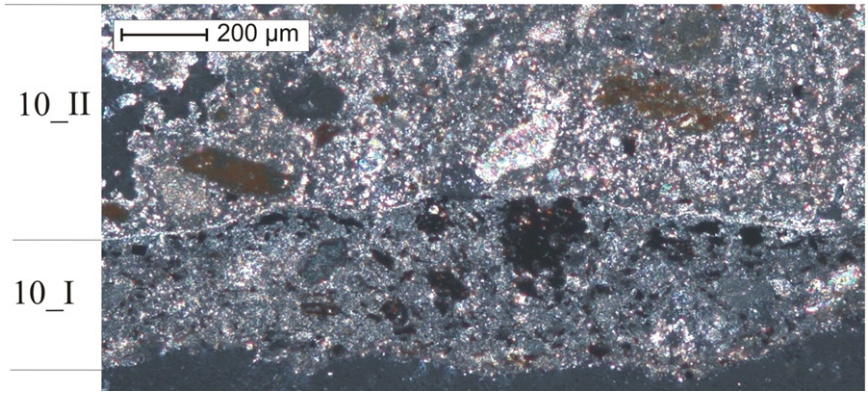

Figure 3 *A microphotograph of sample 10 (crossed polars).*

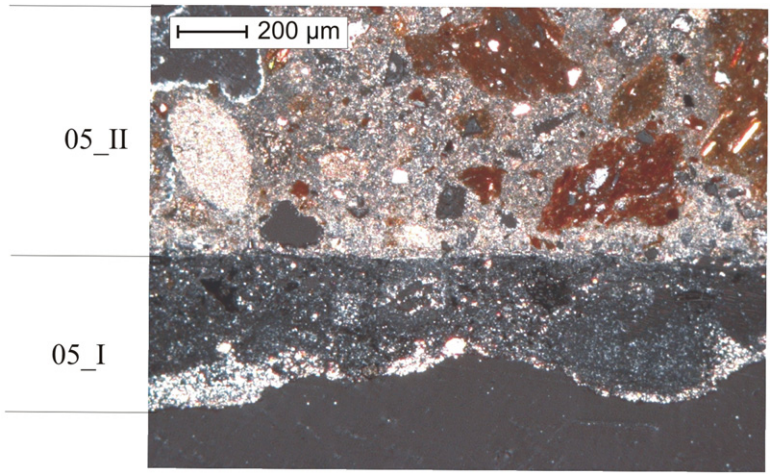

Figure 4 *A microphotograph of sample 05 (crossed polars).*

This basin has the characteristics of a production basin, and was used to produce and/or store wine and oil (Brun 2004; Pecci *et al*. 2013).

Methods

All of the samples were studied in thin section by optical microscopy, using a Zeiss petrographic microscope (Table 2) working between 25 and 400 magnification, and microphotographs were taken using a Zeiss AxioCam Mrc with a 2/3 in CCD sensor. X-ray fluorescence (XRF) on 6 g of pressed powders (maximum working pressure 25 bar) with a boric acid support was used to determine the chemical composition of the major (SiO_2, TiO_2, Al_2O_3, Fe_2O_3, MnO, MgO, CaO, Na_2O, K_2O and P_2O_5) and trace (Ni, Cr, V, La, Ce, Co, Ba, Nb, Y, Sr, Zr and Rb) elements. The chemical elements were analysed with a rhodium tube with 40 kW intensity using a Bruker S8 Tiger WD X-ray fluorescence spectrometer, with an XRF beam of 34 mm. The analytical results are listed in Tables 3 and 4.

Table 2 *Petrographic features on thin sections of mortars*

	By polarized microscopy		*Semi-quantitative visual estimation by polarized microscopy (Ricci Lucchi 1980; Myron Best 2003)*			*By polarized microscopy*				
	Mean aggregate size (mm)	*Maximum aggregate size (mm)*	*% Aggregate (size > 1/16 mm)*	*% Binder (size < 1/16 mm)*	*% Macroporosity (size > 1/16 mm)*	*Mineralogical phases of the aggregate*	*Crushed ceramics*	*Rock fragments (supported by SEM–EDS analysis)*	*Sorting by Jerram* et al. *(1996)*	*Other*
01_I	0.95	4.80	20	78	2	Dol, Ms, Or	No	Dolomitic limestones	M.W.S	–
01_II	1.20	10.50	35	60	5	Qtz, Pl, Dol, Ms, Cal, Bt, Om, Di	Yes	Dolomitic limestones, limestone (traces)	P.S.	–
03	0.57	1.97	1	96	3	Cal, Qtz, Ms	No	Chert and argillites in traces	W.S.	–
04	2.00	4.00	40	55	5	Dol, Qtz	No	Dolomitic limestones	W.S.	–
05_II	1.12	3.00	25	73	3	Qtz, Pl, Dol, Ms, Bt, Om, Di	Yes	Dolomitic limestones	W.S.	Charcoal (traces)
05_I	0.035 (only charcoal)	0.5 (only charcoal)	7	92	2	Dol (traces)	No	Dolomitic limestones (traces)	M.S.	–
06	1.21	4.00	40	59	2	Dol, Qtz	No	Dolomitic rocks and traces of argillites	W.S.	–
07	3.00	12.00	30	68	3	Qtz, Ms, Cal, Pl, Dol, Om	Yes	Dolomitic rocks (traces)	M.S.	–
09	1.20	5.30	38	60	2	Dol, Qtz	No	Dolomitic limestones and traces of argillites	W.S.	
10_II	1.00	2.80	25	72	4	Qtz, Pl, Ms, Bt, Dol, Om	Yes	Dolomitic limestones	W.S.	–
10_I	0.038 (only charcoal)	0.3 (only charcoal)	10	89	2	Dol (traces)	No	Dolomitic limestones (traces)	M.S.	–
11	2.00	8.50	23	75	2	Dol, Cal, Qtz	Yes (traces)	Dolomitic rocks, limestones (traces)	P.S.	Bioclasts (traces)

Bt, biotite; Cal, calcite; Di, diopside; Dol, dolomite; Ms, muscovite; Om, opaque minerals; Or, orthoclase; Pl, plagioclase; Qtz, quartz; M.S., moderately sorted; M.W.S., moderately well sorted; P.S., poorly sorted; W.S., well sorted.

Table 3 *The chemical composition of the major elements of the mortars by XRF analysis*

wt%	SiO_2	TiO_2	Al_2O_3	Fe_2O_3	*MnO*	*MgO*	*CaO*	Na_2O	K_2O	P_2O_5	*L.O.I.*
01_II	39.46	0.60	9.89	3.20	0.05	4.21	19.66	0.32	1.84	0.24	20.54
03	9.77	0.13	1.56	0.55	0.02	2.06	56.43	n.d.	0.31	0.21	28.95
04	1.89	0.05	0.72	0.29	0.01	15.24	37.41	n.d.	0.16	0.03	44.21
05_II	33.29	0.54	7.37	2.65	0.04	2.06	29.80	0.26	1.30	0.27	22.41
06	6.04	0.10	1.42	0.44	0.02	8.00	41.57	n.d.	0.32	0.13	41.96
07	43.62	0.69	12.68	4.44	0.08	3.72	15.93	0.42	2.50	0.21	15.73
09	4.08	0.07	0.86	0.27	0.02	11.08	40.25	n.d.	0.19	0.06	43.13
10_II	33.87	0.51	6.96	2.52	0.05	1.90	29.37	0.25	1.52	0.28	22.78
11	12.79	0.19	3.06	0.90	0.03	5.47	38.48	0.11	0.64	0.14	38.19

L.O.I., loss on ignition; n.d., not detected.

Table 4 *The chemical composition of minor elements of the mortars by XRF analysis*

ppm	*Ni*	*Cr*	*V*	*La*	*Ce*	*Co*	*Ba*	*Nb*	*Y*	*Sr*	*Zr*	*Rb*
01_II	25	54	86	11	44	5	403	12	33	404	141	76
03	9	n.d.	27	n.d.	7	n.d.	36	6	19	471	25	13
04	4	n.d.	17	n.d.	8	n.d.	19	5	8	221	24	12
05_II	19	32	72	4	36	4	210	10	34	520	125	52
06	6	n.d.	28	n.d.	14	n.d.	29	5	14	260	37	17
07	27	78	111	10	61	11	548	12	34	381	141	92
09	6	n.d.	17	n.d.	10	n.d.	n.d.	5	10	365	31	12
10_II	17	29	75	n.d.	39	3	179	11	33	472	122	56
11	12	n.d.	42	n.d.	13	n.d.	114	7	19	333	48	32

n.d., Not detected.

A semi-quantitative estimate of the aggregate/binder ratio and the macroporosity (Table 2) was obtained by comparing the thin sections observed by optical microscopy with charts to aid visual estimation of modal proportions of minerals in rocks (Ricci Lucchi 1980; Myron Best 2003). The binder (size < 1/16 mm), the lumps (Bakolas *et al*. 1995; Barba *et al*. 2009) and the carbonatic rock fragments of the mortars were also analysed on polished thin sections to determine their major chemical composition by scanning electron microscopy with energy-dispersive X-ray spectroscopic (SEM–EDS) microanalysis, using a FEI Quanta 200 instrument equipped with an EDAX Si with Li detector (Tables 5 and 6).

The semi-quantitative mineralogical composition of the samples (Table 7) was studied using a Bruker D8 Advance X-ray powder diffractometer (XRPD) with Cu–K_α radiation, operating at 40 kV and 40 mA. Powder diffraction data were collected in the range 3–60° 2θ in steps of 0.02° 2θ (step time 0.4 s). The EVA software program (DIFFRACplus EVA) was used to identify the mineral phases in each X-ray powder spectrum, by comparing experimental peaks with PDF2 reference patterns.

Table 5 *SEM–EDS microanalysis of the binder (B) and lumps (L) in mortars*

wt%	SiO_2	TiO_2	Al_2O_3	Fe_2O_3	*MnO*	*MgO*	*CaO*	Na_2O	K_2O	P_2O_5
01_I_B1	3.67	n.d.	1.92	n.d.	n.d.	4.73	88.40	0.54	n.d.	0.75
01__I_B2	6.25	n.d.	1.99	n.d.	n.d.	3.33	87.76	0.28	n.d.	0.38
01__I_B3	6.54	n.d.	2.80	n.d.	n.d.	5.05	84.83	0.34	n.d.	0.44
Mean value	5.49	n.d.	2.24	n.d.	n.d.	4.37	87.00	0.39	n.d.	0.52
01__II_B1	45.13	0.30	15.78	15.50	n.d.	5.37	17.92	n.d.	n.d.	n.d.
01_II_B2	58.05	n.d.	17.53	3.48	n.d.	4.92	15.93	0.08	n.d.	n.d.
01_II_B3	33.39	n.d.	8.10	1.05	n.d.	2.16	54.72	0.57	n.d.	n.d.
Mean value	45.52	0.10	13.80	6.68	n.d.	4.15	29.52	0.33	n.d.	n.d.
01_I_L1	1.28	n.d.	0.67	n.d.	n.d.	1.58	95.99	n.d.	n.d.	0.49
03_B1	2.19	n.d.	0.72	n.d.	n.d.	3.20	93.34	0.54	n.d.	n.d.
03_B2	2.32	n.d.	0.99	n.d.	n.d.	2.57	92.75	0.71	n.d.	0.66
03_B3	3.76	n.d.	0.68	n.d.	n.d.	2.92	92.16	0.49	n.d.	n.d.
Mean value	2.76	n.d.	0.80	n.d.	n.d.	2.90	92.75	0.58	n.d.	0.66
03_L1	0.82	n.d.	0.43	n.d.	n.d.	2.83	95.02	0.64	n.d.	0.26
03_L3	1.50	n.d.	0.95	n.d.	n.d.	3.33	93.53	0.23	n.d.	0.46
Mean value	1.16	n.d.	0.69	n.d.	n.d.	3.08	94.28	0.44	n.d.	0.36
04_B1	2.33	n.d.	1.29	n.d.	n.d.	6.05	88.83	0.69	n.d.	0.81
04_B3	6.30	0.50	4.15	2.71	0.19	8.53	76.34	0.27	n.d.	1.02
Mean value	4.32	0.25	2.72	1.36	0.01	7.29	82.59	0.48	n.d.	0.92
04_L1	1.21	n.d.	1.20	n.d.	n.d.	1.51	93.48	1.68	n.d.	0.92
04_L2	2.39	n.d.	1.82	0.57	n.d.	1.48	90.52	2.75	n.d.	0.48
Mean value	1.80	n.d.	1.51	0.29	n.d.	1.50	92.00	2.22	n.d.	0.70
05_II_B1	31.93	0.25	9.67	1.62	0.42	2.99	49.56	1.81	0.37	1.38
05_II_B2	25.32	0.31	10.44	0.72	0.14	3.99	55.80	1.97	0.19	1.11
05_II_B3	34.18	0.21	10.57	0.97	0.20	4.01	46.77	1.84	0.97	0.27
Mean value	30.48	0.26	10.23	1.10	0.25	3.66	50.71	1.87	0.51	0.92
05_II_L1	7.33	n.d.	3.03	0.65	n.d.	2.72	81.73	2.60	0.63	1.31
05_I_B1	11.38	1.12	4.27	1.71	0.26	5.95	68.83	4.19	0.31	1.98
05_I_B2	7.62	0.54	4.49	0.84	n.d.	5.01	73.58	4.90	0.84	2.18
05_I_B3	8.92	0.83	4.13	2.59	0.80	4.23	71.23	4.11	0.54	2.63
Mean value	9.31	0.83	4.30	1.71	0.35	5.06	71.21	4.40	0.56	2.26
06_B1	15.73	0.80	8.32	1.50	0.86	6.84	59.03	3.39	0.83	2.69
06_B3	16.57	n.d.	7.41	2.46	n.d.	8.00	62.81	1.47	0.41	0.87
Mean value	16.15	0.40	7.87	1.98	0.43	7.42	60.92	2.43	0.62	1.78
06_L1	4.04	0.66	2.47	0.56	0.32	3.77	83.17	2.55	0.57	1.89
06_L2	3.27	n.d.	2.81	n.d.	0.00	4.94	82.68	4.22	n.d.	2.08
06_L3	4.33	0.67	3.46	1.09	0.65	4.50	79.12	3.89	0.43	1.86
Mean value	3.88	0.44	2.91	0.55	0.32	4.40	81.66	3.55	0.33	1.94
07_B1	16.47	n.d.	6.85	1.34	0.28	7.49	62.91	2.28	0.54	1.85
07_B2	16.49	0.45	6.05	1.46	0.41	6.60	65.89	1.10	0.54	1.01
07_B3	19.67	n.d.	6.36	3.76	n.d.	12.06	54.78	1.46	0.66	1.24
Mean value	17.54	0.15	6.42	2.19	0.23	8.72	61.19	1.61	0.58	1.37
09_B1	3.23	0.83	3.31	1.38	1.01	3.57	82.47	3.39	n.d.	0.80
09_B2	2.09	0.30	2.37	0.95	0.32	2.23	88.93	1.90	0.29	0.62
09_B3	2.82	n.d.	2.22	0.45	n.d.	3.18	86.30	3.06	0.50	1.47
Mean value	2.71	0.38	2.63	0.93	0.44	2.99	85.90	2.78	0.26	0.96

Table 5 *(Continued)*

wt%	SiO_2	TiO_2	Al_2O_3	Fe_2O_3	*MnO*	*MgO*	*CaO*	Na_2O	K_2O	P_2O_5
10_II_B1	41.04	0.79	10.63	1.56	0.56	4.39	35.65	2.74	1.09	1.55
10_II_B2	36.96	0.34	8.49	0.86	0.39	2.38	46.18	1.78	1.32	1.29
10_II_B3	28.53	1.48	9.46	1.95	1.22	5.50	44.81	3.86	1.38	1.81
Mean value	35.51	0.87	9.53	1.46	0.72	4.09	42.21	2.79	1.26	1.55
10_I_B1	4.04	0.40	0.93	0.91	0.25	1.24	90.73	n.d.	0.35	1.16
10_I_B2	6.89	0.46	3.88	0.89	0.33	6.73	73.12	4.92	0.40	2.38
10_I_B3	6.48	0.53	2.65	1.25	0.76	3.79	80.55	2.85	n.d.	1.14
Mean value	5.80	0.46	2.49	1.02	0.45	3.92	81.47	2.59	0.25	1.56
11_B1	6.35	0.29	2.33	0.96	0.22	1.64	85.42	1.29	0.44	1.05
11_B2	5.59	0.30	2.39	1.23	0.24	1.61	86.23	1.10	0.42	0.88
Mean value	5.97	0.30	2.36	1.10	0.23	1.62	85.83	1.20	0.43	0.97
11_L1	1.79	0.00	1.00	0.44	0.24	1.27	92.91	0.95	0.32	1.08
11_L2	4.04	0.24	1.56	0.34	0.00	1.40	89.86	0.62	0.38	1.57
Mean value	2.91	0.12	1.28	0.39	0.12	1.34	91.38	0.78	0.35	1.32

n.d., Not detected.

Table 6 *SEM–EDS microanalysis of the carbonate rock fragments in mortars*

wt%	SiO_2	TiO_2	Al_2O_3	Fe_2O_3	*MnO*	*MgO*	*CaO*	Na_2O	K_2O	P_2O_5
01__I_R1	1.54	n.d.	0.58	n.d.	n.d.	40.07	57.35	0.32	n.d.	0.13
01_I_R2	3.26	n.d.	0.90	n.d.	n.d.	38.13	57.25	0.47	n.d.	n.d.
01_II_R3	5.48	n.d.	1.66	0.37	n.d.	1.24	90.66	0.20	n.d.	0.40
01__II_R4	4.40	n.d.	1.60	0.18	n.d.	38.63	54.47	0.61	n.d.	0.11
04_R1	1.03	n.d.	0.50	n.d.	n.d.	41.36	56.36	0.57	n.d.	0.18
04_R2	0.39	n.d.	0.22	n.d.	n.d.	41.94	56.51	0.60	n.d.	0.33
05_I_R1	2.46	n.d.	1.65	0.40	0.25	49.67	43.99	0.86	0.09	0.62
06_R1	2.42	0.48	2.10	0.51	0.44	52.10	38.70	2.12	0.21	0.92
06_R2	2.30	0.58	1.94	0.45	0.15	48.79	42.91	2.08	0.00	0.80
06_R3	0.62	0.20	0.99	0.45	0.30	48.13	47.56	1.22	0.19	0.35
07_R1	1.67	n.d.	1.91	0.33	n.d.	52.95	39.76	2.27	n.d.	1.11
09_R1	0.43	0.38	0.53	0.62	0.21	44.90	51.39	0.81	0.12	0.60
09__R2	1.04	n.d.	1.27	0.42	n.d.	46.43	48.74	1.29	n.d.	0.81
09__R3	4.04	0.47	2.56	0.86	0.33	43.84	45.78	1.29	n.d.	0.84
10_II_R1	0.40	0.09	0.45	0.25	0.14	47.10	49.56	1.40	0.20	0.40
10_I_R1	2.00	n.d.	2.42	0.36	0.17	54.13	38.22	2.18	0.25	0.28
11_R1	0.59	0.00	0.31	0.74	0.35	41.64	54.97	0.62	0.11	0.66
11_R2	1.82	0.10	1.31	0.28	0.00	39.47	54.91	0.94	0.17	0.99
11_R3	1.54	0.00	1.15	0.00	0.00	1.47	93.22	1.12	0.26	1.24

n.d., Not detected.

Table 7 *The semi-quantitative mineralogical composition of mortars in order of decreasing relative abundance (as detected by XRPD, SEM–EDS and optical microscopy)*

	By XRPD analysis
	max.----------min.
01_II	Cal, Qtz, Dol, An, Sm, Ms
03	Cal, Qtz, Mul
04	Dol, Cal, Qtz
05_II	Cal, Qtz, Dol, Ms, An
06	Dol, Cal, Qtz
07	Qtz, Cal, Ms, An
09	Dol, Cal, Qtz
10_II	Cal, Qtz, An, Ms, Dol
11	Dol, Cal, Qtz

An, anorthite; Cal, calcite; Dol, dolomite; Ms, muscovite; Mul, mullite; Qtz, quartz; Sm, smectite.

In samples with multiple layers, XRF and XRPD analyses were performed only on the thicker layers (samples 01_II, 05_II and 10_II), because the amount of sample from the thinner layer was too low to obtain representative chemical and mineralogical data.

RESULTS AND DISCUSSION

Petrographic analysis and mineralogical composition of the mortars

The analysed layers of the mortars under study can be divided into two main groups: those without crushed ceramics (samples 01_I, 03, 04, 05_I, 06, 09 and 10_I) and those with crushed ceramics (samples 01_II, 05_II, 07, 10_II and 11). The mean size of the aggregates varies from 0.035 mm for sample 05_II to 3 mm for sample 07 (Table 2 and Fig. 5). Its maximum size is sometimes greater than 1 cm, as in samples 01_II and 07 (Fig. 5). Most of the layers without crushed ceramics (samples 01_I, 04, 06 and 09) have an aggregate that is almost exclusively made of microcrystalline dolomitic limestones (Fig. 6 (a)) with non-planar-anhedral dolomite (Gregg and Sibley 1984; Sibley and Gregg 1987). Frequently, dolomitic limestones have a cryptocrystalline texture (Fig. 6 (b)). Occasionally, in those without crushed ceramics, it is possible to identify the presence of monocrystalline quartz, orthoclase and muscovite. Traces of limestone were found only in samples 01_II and 11, while traces of argillites were found only in samples 03, 06 and 09. The dolomitic composition of the rock fragments was confirmed by the SEM–EDS microanalysis (Fig. 7). In Figure 7, we can see that most rocks have a magnesian composition, except for two fragments in samples 01_II and 11, classified as a limestone. In the layers with aggregate mainly containing crushed ceramics, as well as dolomite, muscovite and the quartz, it is also possible to observe the presence of diopside, biotite, plagioclase and opaque minerals (Tables 2 and 7).

Among the layers without crushed ceramics, samples 05_I and 10_I are distinctive. They represent the thinner layer of the mortars 05 and 10, respectively. These layers have an aggregate composed mainly of charcoal fragments (Figs 6 (c) and 6 (d)), with traces of carbonatic rocks.

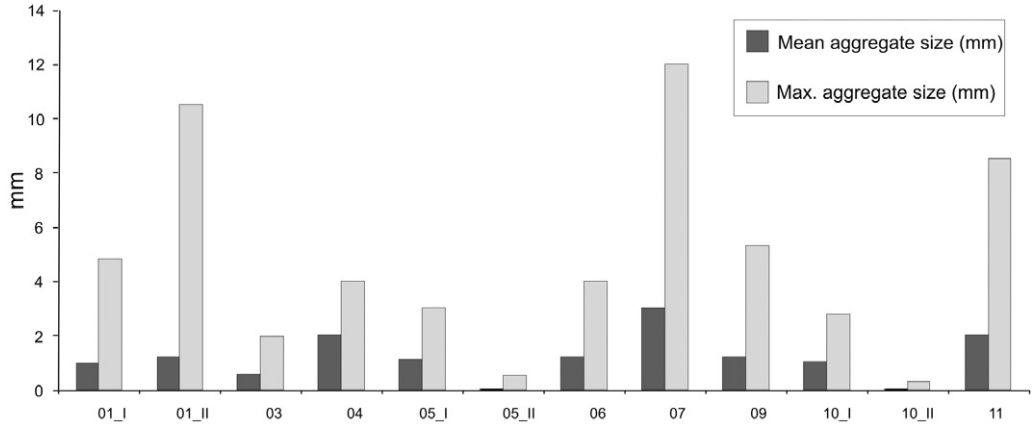

Figure 5 *The mean and maximum size of the aggregate in the mortars.*

Sample 03 is also interesting, as it is the only sample that has approximately 96% of binder (Fig. 8). This sample is the only one in which the presence of dolomite was not detected, while traces of quartz, muscovite, mullite (Table 7) and chert fragments (Fig. 6 (e)) were identified. In layers 01_II and 07, the mean size of the ceramic fragments is higher than in layers 05_II and 10_II (Fig. 5 and Table 2). These layers also have different aggregate/binder ratios (Fig. 8 and Table 2). In sample 11, traces of crushed ceramics and limestone were found. The aggregate is composed mainly of dolomitic microcrystalline and cryptocrystalline rocks. Therefore, the minerals found are dolomite, calcite and quartz (Tables 2 and 7).

Composition of the binder

The study of the binder composition was performed by comparing its chemical composition with that of the lumps inside the same mortar. As a matter of fact, the composition of the lumps is the same as that of the limestone used to produce lime (Bakolas *et al*. 1995; Barba *et al*. 2009). Among the samples analysed in this work, only a few lumps were found in layers 01_I, 03, 04, 05_II, 06 (Fig. 6 (f)) and 11. In the remaining samples, it was only possible to analyse the composition of the binder. The results of the analyses are summarized in Table 5.

Figure 9 shows that all samples with crushed ceramics have $SiO_2 + Al_2O_3 + Fe_2O_3$ contents in the binder ranging from 24.66%, in sample 07, to 79.06%, in sample 01_II. This is due to the initial use of calcium hydroxide (slaked lime), which, mixed with crushed ceramics, underwent an increase of SiO_2, Al_2O_3 and Fe_2O_3 content due to the probable formation of low-crystallinity C-S-H phases (Taylor 1997; Hodgkinson and Hughes 1999; Qing *et al*. 2006). Only in sample 11 is the $SiO_2 + Al_2O_3 + Fe_2O_3$ content relatively low (approximately 9.64%), because in this sample the content of ceramic fragments determined by the petrographic analysis is less than 1%. The sample 05_II is the only mortar with crushed ceramics in which it was possible to identify and analyse a lump. In Figure 9 (d), it is possible to observe that the lump has kept its original composition, as shown by the high $CaO + MgO$ content and the low $SiO_2 + Al_2O_3 + Fe_2O_3$ content.

Another very interesting detail summarized in the data in Table 5 and Figure 9 is that the compositions of the lumps and the binder are compatible with a limestone with a CaO

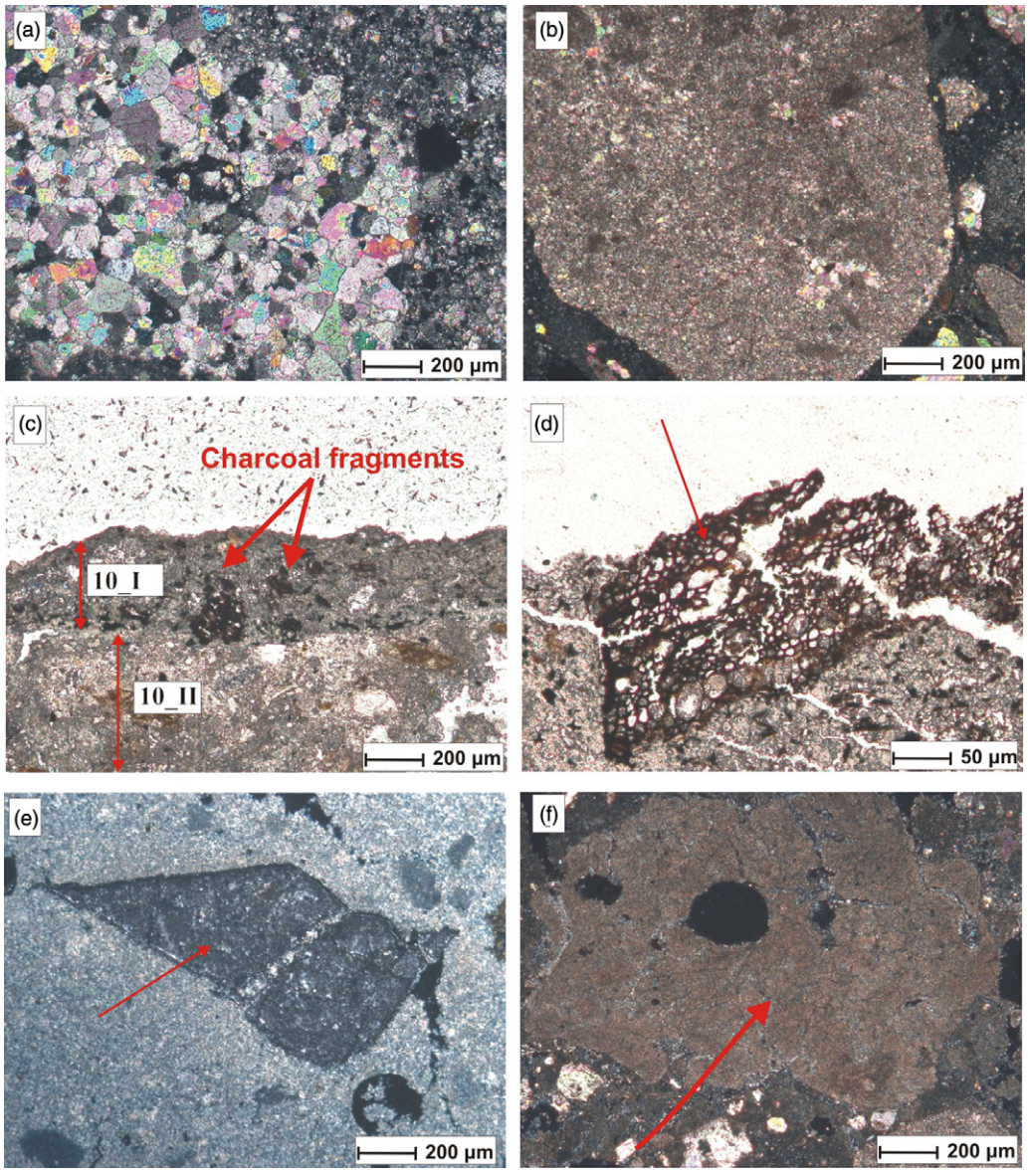

Figure 6 *Microphotographs of mortar aggregate: (a) microcrystalline dolomitic rock in sample 04; (b) cryptocrystalline dolomitic rock in sample 06; (c) sample 10; (d) a charcoal fragment in sample 05_I; (e) a chert fragment in sample 03; (f) a lump in sample 06.*

content higher than ~80%. Theoretically, the high CaO content in lumps may not exclude the use of magnesium limestone in the process of preparation of the lime. As a matter of fact, Chever *et al*. (2010) show that the calcination of dolomitic limestone/dolomite takes place between 510°C and 750°C, a temperature that is considerably lower than that needed to decompose calcitic limestone alone (~900°C). Consequently, when the calcite is well burnt, the dolomite tends to be overburnt. In addition, we can find high-calcium lime lumps in magnesian

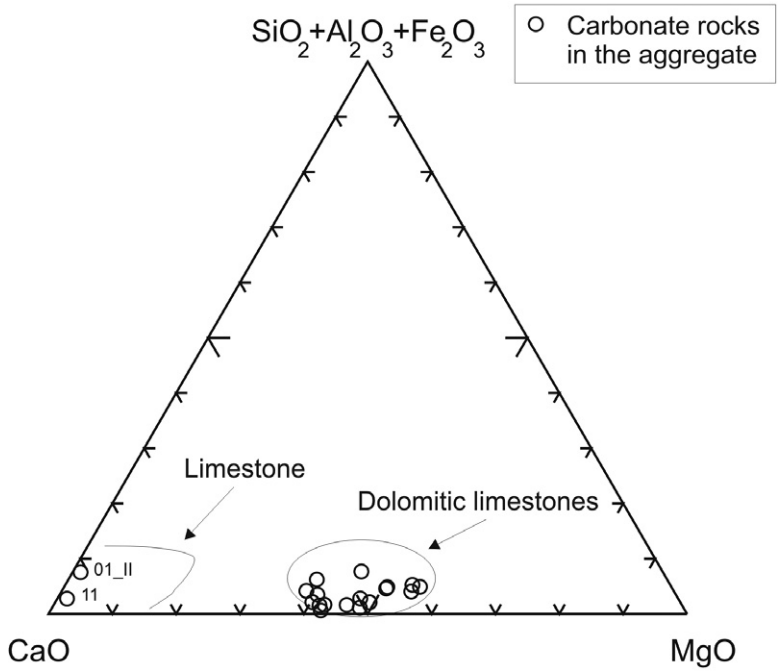

Figure 7 *The composition of the carbonate rocks in mortars by SEM–EDS analysis.*

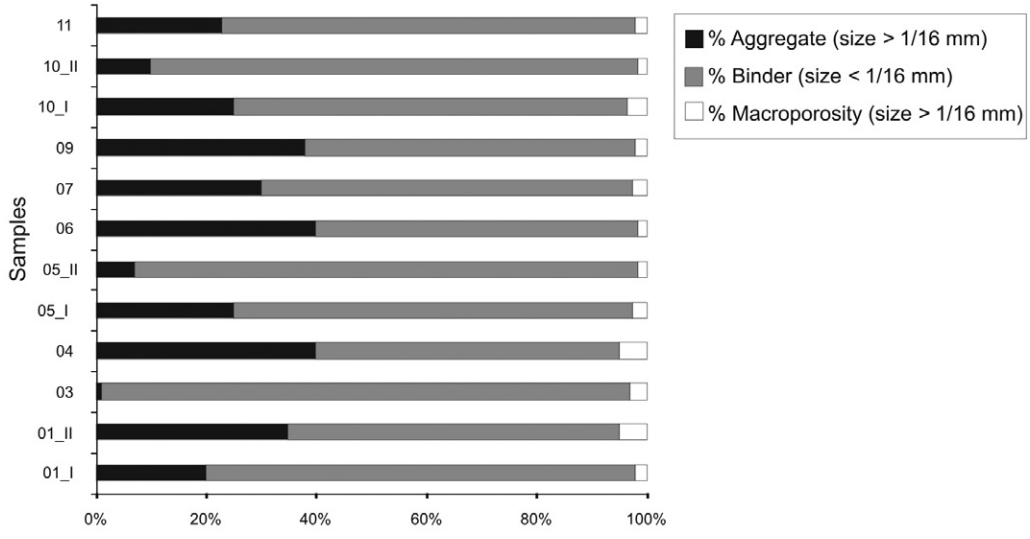

Figure 8 *A semi-quantitative estimate of the modal content of aggregate, binder and macroporosity in mortars.*

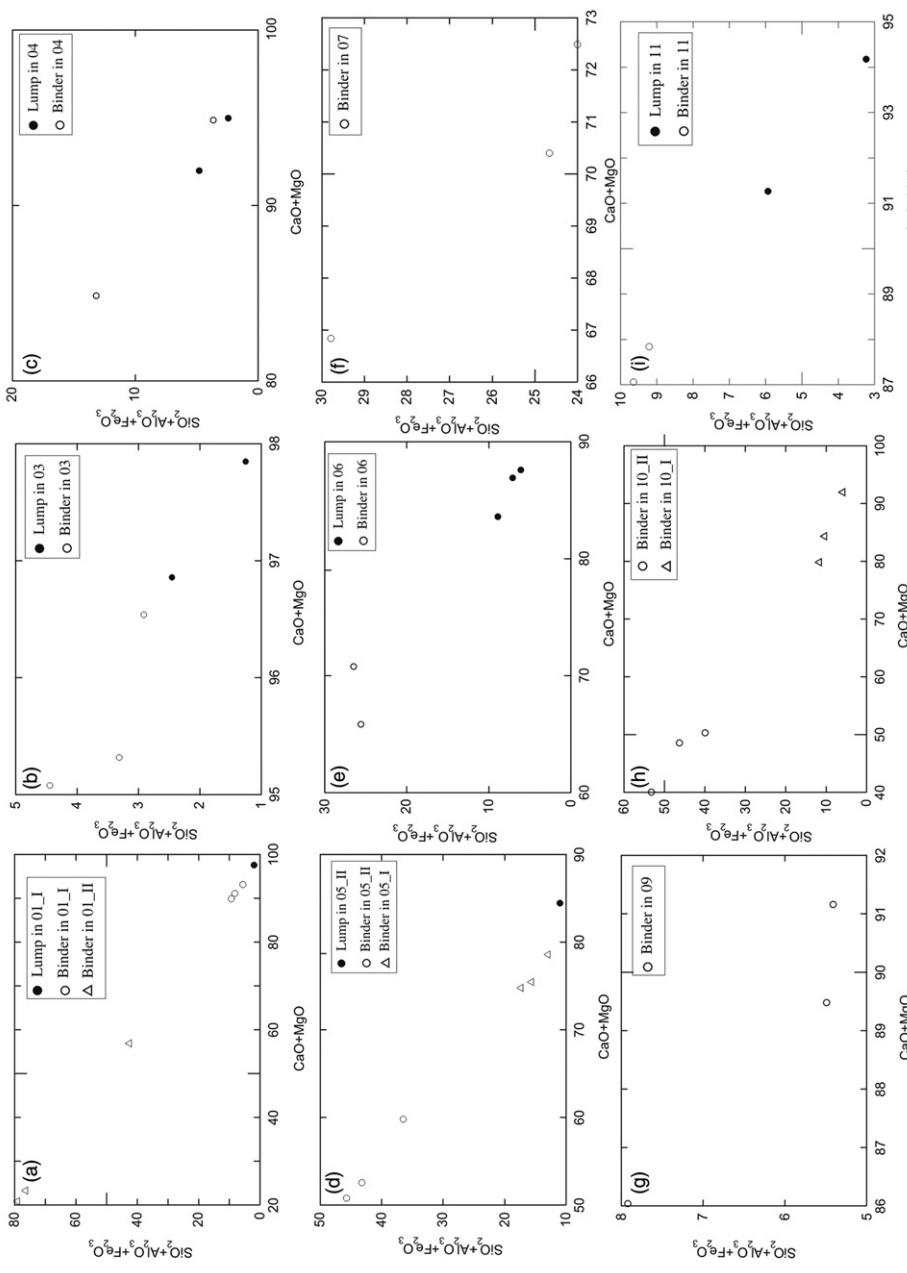

Figure 9 *$SiO_2 + Al_2O_3 + Fe_2O_3$ versus CaO + MgO diagrams of the binder (open symbols) and lumps (solid black symbols) in the mortars by SEM–EDS analysis: (a) samples 01_I and 01_II; (b) sample 03; (c) sample 04; (d) samples 05_I and 05_II; (e) sample 06; (f) sample 07; (g) sample 09; (h) samples 10_I and 10_II; (i) sample 11.*

lime mortars, which are carbonate rock fragments that have not been completely burned. However, we discard the explanation proposed by Chever et al. (2010), because the lumps analysed in this work have a shape, morphology and microtexture compatible with lumps formed during the slaking of the lime (Fig. 6). Therefore, they are not carbonate rock fragments that have not been completely burned during the calcination process. Furthermore, the hypothesis of the use of limestone with a CaO content higher than ~80% in the production process of the lime is supported by the fact that not only are the lumps low in magnesium, but also the binder.

Chemical and petrographic similarities among the samples

A combination of all the data collected highlights a strong compositional similarity between samples 10 and 05. Both samples are chemically very similar (Figs 10 (a) and 10 (b)) and they are made of crushed ceramics. They also have a compatible aggregate/binder ratio (Fig. 8), as well as compatible sorting (Table 2) and mean size of the aggregates (Fig. 5). The mortars 10 and 05 are also the only multi-layer samples that have a thin layer (Samples 10_I e 05_I), with a thickness of ~200 μm, in which the aggregate is predominantly made of charcoal. This suggests that they belong to the same construction phase or even to the same basin. Also very similar are samples 06 and 09. The aggregate is composed mainly of cryptocrystalline and microcrystalline dolomitic limestones in a 1:1 ratio. Sample 06 comes from a plastered cover of a tomb from sector W, room II, while sample 09 comes from a floor in the northern room of the baptistery (Fig. 1). The analytical data suggest that they belong to the same construction phase. Sample 04 differs from samples 06 and 09 due to the fact that carbonatic microcrystalline fragments are more abundant than the cryptocrystalline ones; while in samples 06 and 09 the carbonatic cryptocrystalline fragments exceed the microcrystalline fragments. These data suggest the use of aggregates coming from different outcrops. Sample 03 is the only mortar in which dolomite was not detected by OM and XRPD analyses and shows the highest content of binder (Fig. 8). Although samples 07 and 01_II are chemically similar (Figs 10 (a) and 10 (b)), they differ in the mean size of the aggregate (higher in sample 07) and in the sorting (lower in sample 01_II). Mortar 11 can be considered as different from the other samples because it is the only mortar that contains relatively scarce crushed ceramics and it has a content of aggregate of ~23%, which consists mainly of carbonate rock fragments (Table 2).

CONCLUSIONS

The study of the mortars recovered at Son Peretó reveals some similarities between the samples; in particular, between samples 10 and 05, and between samples 06 and 09. Many of the analysed samples have an aggregate composed mainly of dolomitic limestones with a high MgO content, ranging between 38.13% and 52.95% (Table 6). This type of rock can be used for the production of lime, as previous papers have shown (Bruni *et al*. 1998; Cagnana and Mannoni 2000; Montoya *et al*. 2003; Rampazzi *et al*. 2006; Chever *et al*. 2010). Nevertheless, the SEM–EDS analyses performed on the binder and lumps of the samples from Son Peretó do not reveal the use of these rocks (Fig. 9 and Table 5). The lime was, in fact, produced in all cases by calcining a limestone that has a very high CaO content (~80%). The local geology has both typologies of rocks (Álvaro López *et al*. 1991), but it was probably easier to use the limestone with 80% of CaO because its

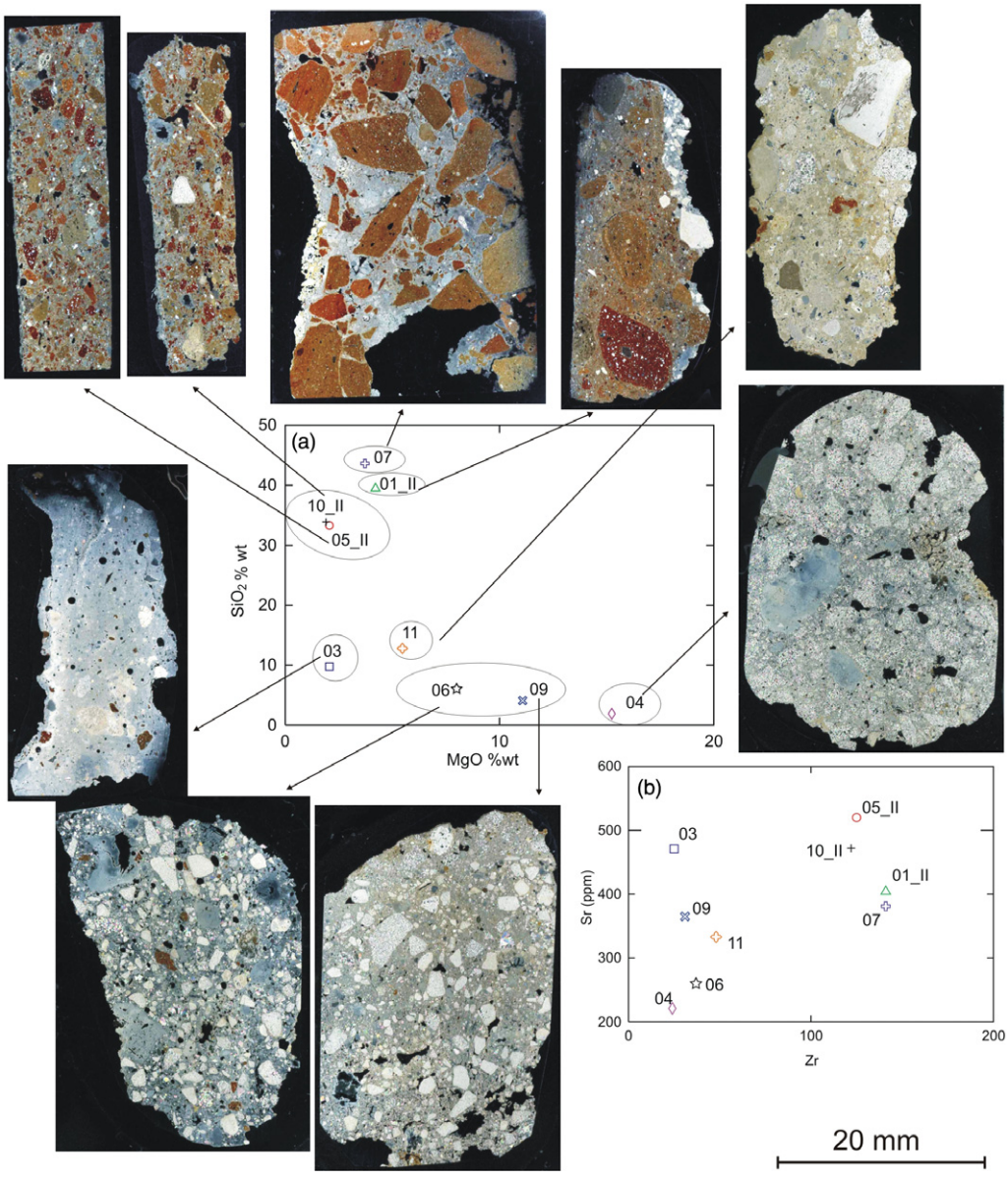

Figure 10 *(a) An MgO versus SiO_2 diagram and flatbed scan image of the mortars under polarized light: the ellipse encloses the samples that have the same chemical and petrographic features. (b) A Zr versus Sr diagram.*

quarry was nearest to the archaeological site. However, to definitively clarify this question, studies on the provenance of the raw materials used to prepare the mortars will be the objective of our future work.

In the mortars with an aggregate mainly composed of dolomitic limestone fragments, it is possible to detect the use of two types of aggregate: the first type is predominantly made of

cryptocrystalline dolomitic limestones (in sample 04 only); while the second consists of microcrystalline and cryptocrystalline dolomitic limestones in a 1:1 ratio (in samples 06 and 09).

In general, it is worth observing that the baptismal basins (samples 10, 01), which had to contain water, were coated with a mortar made of crushed ceramics mixed with lime, which was used because of its hydraulic properties. Also, sample 05, which possibly belongs to a baptismal basin, is made of crushed ceramics mortar. The presence of layers 10_I and 05_I (inner layers of samples 10 and 05), which are almost exclusively made of charcoal, is also of interest because of their compositional singularity. A mention of the use of charcoal in the making of mortars can be found in Book 36, Chapter 63 of Plinius' *Naturalis historia* (1987), when the author speaks about a particular type of floor:

> We must not omit here one other kind of pavement, that known as the 'Graecanic'. The ground is well rammed down, and a bed of rough work, or else broken pottery, is then laid upon it. Upon the top of this, a layer of charcoal is placed, well trodden down with a mixture of sand, lime, and ashes; care being taken, by line and rule, to give it a uniform thickness of half a foot. The surface then presents the ordinary appearance of the ground; but if it is well rubbed with the polishing-stone, it will have all the appearance of a black pavement.

The reason for the use of charcoal at Son Peretó is still unclear, although it may have been used to improve the waterproofing qualities of the mortar.

Samples 01 (small baptismal basin) and 10 (large baptismal basin) are clearly different. Moreover, the similarities between samples 05 and 10 are evident, as shown by both the chemical and the petrographic analyses. These observations are very interesting from an archaeological point of view. In fact, sample 10 belongs to the so-called large baptismal basin, while sample 05 is a fragment of mortar found under the small baptismal basin. The results of the analyses suggest that mortars 05 and 10 belong to the same building phase. The strong compositional similarities between the two samples support the hypothesis that sample 05 belonged to the large baptismal basin itself. The latter may have been partially destroyed and the rubble deposited as a construction level for the small basin. This statement supports the idea that the small basin substituted for the larger one, probably due to a change in the baptismal ritual, which evolved from immersion of adults to children's baptism, or other practices that did not require the use of a deep basin. This interpretation contributes to solving the archaeological problem posed by the possible coexistence of the two baptismal basins in the same church, indicating that the two baptismal fonts were not used together; thus closing the long archaeological debate that these baptismal fonts have generated since their discovery.

As stated above, samples 06 and 09 are also very similar mortars, and this suggests that they were made during the same construction phase. This is important in archaeological terms because sample 06 comes from the plastered cover of a tomb in sector W, room II, for which the ceramic study provides a *post quem* dating of around AD 500 and, therefore, at least in the sixth century AD. Therefore, the analytical results for these mortars suggest a similar dating for the remains of a floor (09) found in the baptistery and in tomb (06) of sector W. In this phase, a necropolis stretched across the West Sector was linked to both the church and the baptistery. At a later date, some rooms were built over this necropolis, and they were used until the destruction of the site, probably at the very beginning of the eighth century.

Samples 03 and 07 do not show any similarities, thus pointing out that the infilling of burial 2008-6 was made with mortars that came from different construction phases. Sample 04 does not show any similarities with any other mortar, and thus does not allow us—for the moment—to relate the cover of the tomb found under the wall that divides the central and northern rooms of

the baptistery to any other part of the site. Sample 11 is also different from all of the others, probably due to the characteristics of the basin from which it was taken, in that was used for the production or storage of wine and oil.

Besides providing important information on the technological know-how of those who participated in the construction of the buildings of Son Peretó, the data obtained by means of the analyses of the mortars found in this Late Antique site have contributed to the study of its construction phases, to solve the problem of the two baptismal fonts, and will also help in the reproduction of compatible mortars for future restoration works. In particular, the study shows how a well-targeted, although relatively small-scale, sampling can solve a very important archaeological question with historical implications.

ACKNOWLEDGEMENTS

Part of this work was performed in the framework of the project 'Production, trade and consumption of food in Late Antiquity', PIEF-GA-2009-235863, funded by the Marie Curie actions, and of the project LRCWMED (HAR200908290/HIST) and CARE-Hispania (HAR2009-13104), funded by the Spanish Ministerio de Ciencia e Innovación, Subdirección General de Proyectos de Investigación, with the contribution of the European Regional Development Fund. This is part of the activities of the Equip de Recerca Arqueològica i Arqueomètrica de la Universitat de Barcelona (ERAAUB) (SGR2009-1173), thanks to the support of the DIUE Generalitat de Catalunya. We are indebted to the Consell de Mallorca and Ajuntament de Manacor for financial support of the framework programme of archaeological excavations at the site of Son Peretó. Finally, we are grateful to M. Salas for helping in the collection of the samples and in the administrative duties.

REFERENCES

Aguiló, J., 1923, Un descubrimiento arqueológico en Manacor y un nuevo argumento de la ortodoxia final del Grande Osio de Córdoba, *Butlletí de la Societat Arqueològica Lul·liana*, **19–20**, 204–7.

Alcaide, S., 2011, *Arquitectura cristiana balear en la antigüedad tardía (ss. V–X d.C)*, Tesis doctoral, Universitat Rovira i Virgili, Tarragona (http://www.tesisenred.net/handle/10803/32933).

Álvaro López, M., Del Olmo Zamora, P., Ramírez Del Pozo, J., and Sabat Montserra, F., 1991, *Manacor: mapa geológico de España escala 1:50.000*, Instituto Tecnológico Geominero de España, Madrid.

Anastasiou, M., Hasapis, Th., Zorba, T., Pavlidou, E., Chrissafis, K., and Paraskevopoulos, K. M., 2006, TG–DTA and FTIR analyses of plasters from Byzantine monuments in Balkan region—comparative study, *Journal of Thermal Analysis and Calorimetry*, **84**, 27–32.

Bakolas, A., Biscontin, G., Moropoulou, A., and Zendri, E., 1995, Characterization of the lumps in the mortars of historic masonry, *Thermochimica Acta*, **269/270**, 809–16.

Bakolas, A., Biscontin, G., Moropoulou, A., and Zendri, E., 1998, Characterization of structural Byzantine mortars by thermogravimetric analysis, *Thermochimica Acta*, **321**, 151–60.

Barba, L., Blancas, J., Manzanilla, L. R., Ortiz, A., Barca, D., Crisci, G. M., Miriello, D., and Pecci, A., 2009, Provenance of the limestone used in Teotihuacan (Mexico): a methodological approach, *Archaeometry*, **51**, 525–45.

Brun, J. P., 2004, *Archaeologie du vin et de l'huile dans l'Empire romain*, Editions Errance, Paris.

Bruni, S., Cariati, F., Fermo, P., Pozzi, A., and Toniolo, L., 1998, Characterization of ancient magnesian mortars coming from northern Italy, *Thermochimica Acta*, **321**, 161–5.

Cagnana, A., and Mannoni, T., 2000, *Archeologia dei materiali da costruzione*, Società Archeologica Padana, Mantova.

Carò, F., Riccardi, M. P., and Mazzilli Savini, M. T., 2008, Characterization of plasters and mortars as a tool in archaeological studies: the case of Lardirago Castle in Pavia, northern Italy, *Archaeometry*, **50**, 85–100.

Chever, L., Pavía, S., and Howard, R., 2010, Physical properties of magnesian lime mortars, *Materials and Structures*, **43**, 283–96.

Crisci, G. M., and Miriello, D., 2006, I materiali del costruito tradizionale: un mondo ancora in gran parte da scoprire, in *Proceedings of the Associazione Italiana di Archeometria, Ravello, 6–7 February 2003* (eds. G. M. Crisci and C. Gattuso), 107–12, Edipuglia, Bari.

Crisci, G. M., Franzini, M., Lezzerini , M., Mannoni, T., and Riccardi, M. P., 2004, Ancient mortars and their binder, *Periodico di Mineralogica*, **73**, 259–68.

Crisci, G. M., Davoli, M., De Francesco, A. M., Gagliardi, F., Mercurio, P., and Miriello, D., 2001, L'analisi composizionale delle malte: metodo di studio delle fasi costruttive in architettura, *Arkos*, **4**, 36–41.

Duval, N., 1994, La place des églises des Baléars dans l'archéologie Chrétienne de la Méditerranée Occidentale, in *Proceedings de la III Reunión de Arqueología Cristiana Hispánica (Mahón, 1988)*, 203–12, Institut d'Estudis Catalans, Universitat de Barcelona, Consell Insular de Menorca, Barcelona.

Godoy, C., 1989, Arquitectura cristiana y liturgia: reflexiones en torno a la interpretación funcional de los espacios. *Espacio, Tiempo y Forma, Serie I Prehistoria y Arqueología*, **2**, 355–88.

Godoy, C., 1995, *Arqueología y liturgia: iglesias hispánicas (siglos IV al VIII)*, Universitat de Barcelona, Barcelona.

Gregg, J. M., and Sibley, D. F., 1984, Epigenetic dolomitization and the origin of xenotopic dolomite texture, *Journal of Sedimentary Research*, **54**, 908–31.

Hodgkinson, E. S., and Hughes, C. R., 1999, The mineralogy and geochemistry of cement/rock reactions: high-resolution studies of experimental and analogue materials, in *Chemical containment of waste in the geosphere* (eds. R. Metcalfe and C. A. Rochelle), 157, 195–211, Geological Society, London.

Iordanidis, A., Garcia-Guinea, J., Strati, A., Gkimourtzina, A., and Papoulidou, A., 2011, Thermal, mineralogical and spectroscopic study of plasters from three post-Byzantine churches from Kastoria (northern Greece), *Journal of Thermal Analysis and Calorimetry*, **103**(2), 577–86.

Iturgáiz, D., 1963, Baptisterio doble de la basílica de Son Peretó, *Rivista di Archeologia Cristiana*, **39**, 279–87.

Jerram, D. A., Cheadle, M. J., Hunter, R. H., and Elliott, M. T., 1996, The spatial distribution of grains and crystals in rocks, *Contributions to Mineralogy and Petrology*, **125**, 60–74.

Meir, I. A., Freidin, C., and Gilead, I., 2005, Analysis of Byzantine mortars from the Negev Desert, Israel, and subsequent environmental and economic implications, *Journal of Archaeological Science*, **32**, 767–73.

Miriello, D., and Crisci, G. M., 2006, Image analysis and flatbed scanners: a visual procedure in order to study the macro-porosity of the archaeological and historical mortars, *Journal of Cultural Heritage*, **7**, 186–92.

Miriello, D., Bloise, A., Crisci, G. M., Apollaro, C., and La Marca, A., 2011a, Characterisation of archaeological mortars and plasters from Kyme (Turkey), *Journal of Archaeological Science*, **38**, 794–804.

Miriello, D., Bloise, A., Crisci, G. M., Barrese, E., and Apollaro, C., 2010a, Effect of milling: a possible factor influencing the durability of historical mortas, *Archaeometry*, **52**, 668–79.

Miriello, D., Barca, D., Crisci, G. M., Barba, L., Blancas, J., Ortiz, A., Pecci, A., and Lopez Luján, L., 2011b, Characterization and provenance of lime plasters from the Templo Mayor of Tenochtitlan (Mexico City), *Archaeometry*, **53**, 1119–41.

Miriello, D., Barca, D., Bloise, A., Ciarallo, A., Crisci, G. M., De Rose, T., Gattuso, C., Gazineo, F., and La Russa, M.F., 2010b, Characterisation of archaeological mortars from Pompeii (Campania, Italy) and identification of construction phases by compositional data analysis, *Journal of Archaeological Science*, **37**, 2207–23.

Montoya, C., Lanas, J., Arandigoyen, M., Navarro, I., Garcia Casado, P. J., and Alvarez, J. I., 2003, Study of ancient dolomitic mortars of the church of Santa Maria de Zamarce in Navarra (Spain): comparison with simulated standards, *Thermochimica Acta*, **398**, 107–22.

Moropoulou, A., Bakolas, A., and Bisbikou, K., 1995, Characterization of ancient, Byzantine and later historic mortars by thermal and X-ray diffraction techniques, *Thermochimica Acta*, **269/270**, 779–95.

Moropoulou, A., Polikreti, K., Bakolas, A., and Michailidis, P., 2003, Correlation of physicochemical and mechanical properties of historical mortars and classification by multivariate statistics, *Cement and Concrete Research*, **33**, 891–8.

Myron Best, G., 2003, *Igneous and metamorphic petrology*, 2nd edn, Blackwell, Oxford.

Palol, P., 1967, *Arqueología cristiana de la España romana. Siglos IV–VI, CSIC*, Instituto Enrique Flórez, Madrid.

Palol, P., 1994, L'Arqueologia cristiana hispànica després del 1982, in *Proceedings de la III Reunión de Arqueología Cristiana Hispánica (Mahón, 1988)*, 3–40, Institut d'Estudis Catalans, Universitat de Barcelona, Consell Insular de Menorca, Barcelona.

Palol, P., Alomar, A., Camps, J., and Rosselló, G., 1967, Notas sobre las basílicas de Manacor en Mallorca, *Boletín del Seminario de Estudios de Arte y Arqueología*, **33**, 5–45.

Pecci, A., Giorgi, G., Salvini, L., and Cau Ontiveros, M. Á., 2013, Identifying wine markers in ceramics and plasters with gas chromatography–mass spectrometry: experimental, ethnoarchaeological and archaeological materials, *Journal of Archaeological Science*, **40**, 109–15.

Plinius S. G., 1987, *The natural history of Pliny*, trans. J. Bostock and H. T. Riley, Taylor and Francis, London.

Qing, Y., Zenall, Z., Sheng L., and Rongshen, C., 2006, A comparative study on the pozzolanic activity between nano-SiO_2 and silica fume, *Journal of the Wuhan University of Technology—Materials Science Edition*, **21**, 153–7.

Rampazzi, L., Pozzi, A., Sansonetti, A., Toniolo, L., and Giussani, B., 2006, A chemometric approach to the characterisation of historical mortars, *Cement and Concrete Research*, **36**, 1108–14.

Regev, L., Zukerman, A., Hitchcock, L., Maeir, A. M., Weiner, S., and Boaretto, E., 2010, Iron Age hydraulic plaster from Tell es-Safi/Gath, Israel, *Journal of Archaeological Science*, **37**, 3000–9.

Riccardi, M. P., Lezzerini, M., Carò, F., Franzini, M., and Messiga, B., 2007, Microtextural and microchemical studies of hydraulic ancient mortars: two analytical approaches to understand pre-industrial technology processes, *Journal of Cultural Heritage*, **8**, 350–60.

Ricci Lucchi, F., 1980, *Sedimentologia parte I: materiali e tessiture dei sedimenti*, Clueb, Bologna.

Riera Rullan, M., Cau, M. A., Alcaide, S., Salas, M., and Munar, M., 2010, Son Peretó (Mallorca—Baleares), el tiempo de los 'bárbaros'. Pervivencia y transformación en Galia e Hispania (ss. V–VI D.C.), *Zona Arqueológica, Alcalá de Henares,* **11**, 597–9.

Riera Rullan, M., Salas, M., Munar, M., Alcaide, S., and Cau, M. A., 2006, El proyecto de revisión y adecuación del yacimiento de Son Peretó (Manacor, Mallorca, islas Baleares), *Bulletin de la Association pour l'Antiquité Tardive*, **15**, 69–75.

Sibley, D. F., and Gregg, J. M., 1987, Classification of dolomite rock textures, *Journal of Sedimentary Research*, **57**, 967–75.

Taylor, H. F. W., 1997, *Cement chemistry*, 2nd edn, Thomas Telford, London.

Vendrell-Saz, M., Alarcóv, S., Molera, J., and García-Vallés, M., 1996, Dating ancient lime mortars by geochemical and mineralogical analysis, *Archaeometry*, **38**, 143–9.